

Incremental Learning in Semantic Segmentation from Image Labels

Fabio Cermelli^{1,2}, Dario Fontanel¹, Antonio Tavera¹, Marco Ciccone¹, Barbara Caputo¹

¹Politecnico di Torino, ²Italian Institute of Technology

{first.last}@polito.it

Abstract

Although existing semantic segmentation approaches achieve impressive results, they still struggle to update their models incrementally as new categories are uncovered. Furthermore, pixel-by-pixel annotations are expensive and time-consuming. This paper proposes a novel framework for Weakly Incremental Learning for Semantic Segmentation, that aims at learning to segment new classes from cheap and largely available image-level labels. As opposed to existing approaches, that need to generate pseudo-labels offline, we use an auxiliary classifier, trained with image-level labels and regularized by the segmentation model, to obtain pseudo-supervision online and update the model incrementally. We cope with the inherent noise in the process by using soft-labels generated by the auxiliary classifier. We demonstrate the effectiveness of our approach on the Pascal VOC and COCO datasets, outperforming offline weakly-supervised methods and obtaining results comparable with incremental learning methods with full supervision.

1. Introduction

Semantic segmentation is a fundamental problem in computer vision where significant progress has been made thanks to the surge of deep learning [13–15] and the availability of large-scale human-annotated or synthetic datasets [4, 17, 23, 40, 54]. Despite the fact that many pre-trained models using public datasets are available online, one of their key disadvantages is that they are not meant to be incrementally updated over time and their knowledge is often limited to the predefined set of classes.

A naïve solution to this problem would be to extend existing datasets with new annotated samples and train new models from scratch. However, this approach is impractical in case of frequent updates because training on the entire augmented dataset would take too long, increasing the energy consumption and carbon footprint of machine learning models [50, 57, 60]. Moreover, retraining or fine-tuning becomes infeasible when the original data is no longer available, e.g., due to privacy concerns or intellectual property.

A better solution is to incrementally add new classes to

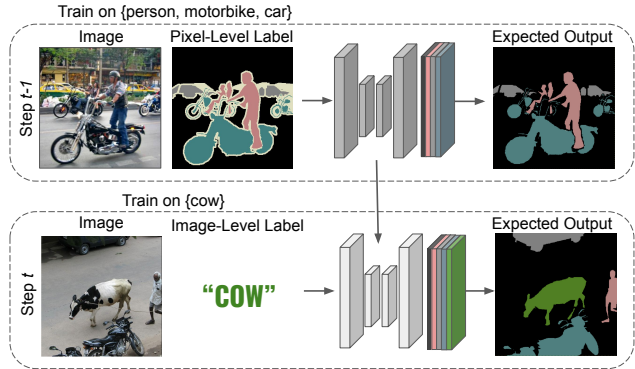


Figure 1. Illustration of WILSS. A model is first pre-trained on a set of classes (e.g., *person*, *motorbike*, *car*), using expensive pixel-wise annotations. Then, in the following incremental learning steps, the model is updated to segment new classes (e.g., *cow*) being provided image-level labels and without access to old data.

the pre-existing model, as done in some recent works [8, 21, 42, 44, 45]. Incremental learning approaches update the model’s parameters by training only on new data and employing ad-hoc techniques to avoid catastrophic forgetting on old classes [43]. While they reduce the cost of training, they rely on pixel-wise supervision on novel classes, which is expensive and time-consuming to collect, and usually requires expert human annotators [6, 40].

To reduce the annotation cost, different types of weak supervision have been proposed: bounding boxes [18, 32], scribbles [39, 61], points [16], and image-level labels [34, 49, 51]. Image labels can be easily retrieved from image classification benchmarks [19] or the web, dramatically lowering the annotation cost. Nevertheless, their use has never been investigated in an incremental learning setting.

In light of these considerations, we argue that it is crucial to jointly address the problems of incrementally updating the model and reducing the annotation cost of new data for semantic segmentation. To this end, we propose to incrementally train a segmentation model using only image-level labels for the new classes. We call this task *Weakly-Supervised Incremental Learning for Semantic Segmentation* (WILSS). This novel setting combines the advantages of incremental learning (training only on new class data)

and weak supervision (cheap and largely available annotations). An illustration of WILSS is reported in Fig. 1.

Directly applying existing weakly-supervised methods to incremental segmentation would require to (i) extract pixel-wise pseudo-supervision offline using a weakly supervised approach [3, 5, 36, 58, 62] and (ii) update the segmentation network resorting to an incremental learning technique [8, 21, 42]. However, we argue that generating pseudo-labels offline in incremental settings is sub-optimal, as it involves two separate training stages and ignores the model’s knowledge on previous classes that can be exploited to learn new classes more efficiently.

Hence, we propose a **Weakly Incremental Learning** framework for semantic Segmentation that incrementally trains a segmentation model generating **ON**line pseudo-supervision from image-level annotations (WILSON) and exploits previous knowledge to learn new classes. We extend a standard encoder-decoder segmentation architecture [13–15] by introducing an auxiliary classifier on the encoder, from which we extract pseudo-supervision for the segmentation backbone. To improve the pseudo-supervision, we train the auxiliary classifier with a pixel-wise loss guided by the predictions of the segmentation model. This regularization serves two purposes: i) it acts as a strong prior for the previous class distribution, informing the model on where old classes are located in the image, and (ii) it provides a saliency prior for extracting better object boundaries. To address the noise present in the pseudo-supervision, instead of using hard pseudo-labels as in previous works [5, 36, 62], we obtain soft-labels from the auxiliary classifier, which provides information on the probability assigned to a pixel to belong to a certain class.

To summarize, the contributions are as follows:

- We propose the Weakly supervised Incremental Learning for Semantic Segmentation (WILSS) task to extend pre-trained segmentation models with new classes using image-level supervision only.
- We propose WILSON, a novel framework that generates pseudo-supervision online using a simple auxiliary classifier trained with an image-level classification loss and a pixel-wise localization loss that relies on old class knowledge. To model the noise in the pseudo-supervision, we use a convex combination of soft and hard labels that improves the segmentation performance over hard labels only.
- We evaluate our method on the Pascal VOC [23] and COCO [40] datasets, showing that our approach outperforms offline weakly-supervised methods, and that it is comparable or slightly inferior w.r.t. fully supervised incremental learning methods.¹

2. Related work

Incremental learning semantic segmentation. Incremental learning (IL) aims at addressing the phenomenon known as *catastrophic forgetting* [25, 43]: a model, expanding its knowledge with new classes over time, gradually forgets previously learned ones. Even if in image classification it has been exhaustively studied [1, 11, 20, 22, 24, 30, 38, 41, 53, 56, 67], in semantic segmentation it is still in its early stages [8, 9, 21, 33, 42, 44–46]. As first shown by [8], catastrophic forgetting in segmentation is exacerbated by the background shift problem; hence, they proposed a modified version of the traditional cross-entropy to propagate only the probability of old classes through the incremental steps and a distillation term to preserve previous knowledge. Later, [21] proposed to preserve long and short-range spatial relationships at feature level, while [45] regularized the latent space to improve class-conditional features separations. Alternatively, [42] used samples of old classes with replay methods to mitigate forgetting. Finally, [9] proposed the incremental few-shot segmentation setting, where only a few images to learn new classes are provided.

Differently from these works, we focus on a more challenging scenario where the supervision on new classes is provided as cheap image-level labels.

Weakly supervised semantic segmentation. Collecting accurate pixel-wise annotations for supervising semantic segmentation models is generally costly and time-consuming. To address this issue, Weakly Supervised Semantic Segmentation (WSSS) methods aim to obtain effective segmentation models using cheaper supervisions such as bounding boxes [18, 32, 48], scribbles [39, 59], points [6, 52], and image-level labels [31, 34, 35, 58]. Because of low prices and large availability on the web, image-level supervision gained the most attention over other types of weak supervision. Most image-based weakly supervised approaches [2, 3, 10, 31, 34, 35, 47, 58] use a two-stage procedure: (i) they generate pixel-wise pseudo-labels and then (ii) use them for training a segmentation backbone. The pseudo-labels are often extracted from an image-level classifier exploiting its Class Activation Maps (CAMs) [66]. An exception is [5], which proposes to learn a segmentation model in a single stage. Previous works focused on improving the pseudo-labels through multiple refinements steps [2, 3], additional losses [5, 10, 31, 34, 58, 62], or erasing techniques that force the CAM to expand and focus on non-discriminative parts of the image [12, 29, 63]. Finally, a recent trend uses external information, such as saliency, to improve the object boundaries [36, 65].

Despite the rapid development of pseudo-labels generation techniques from image-level supervision, these works operate in a static scenario where the model learns from a fixed set of classes. Instead, we focus on the more challeng-

¹Code to replicate our results will be released upon acceptance.

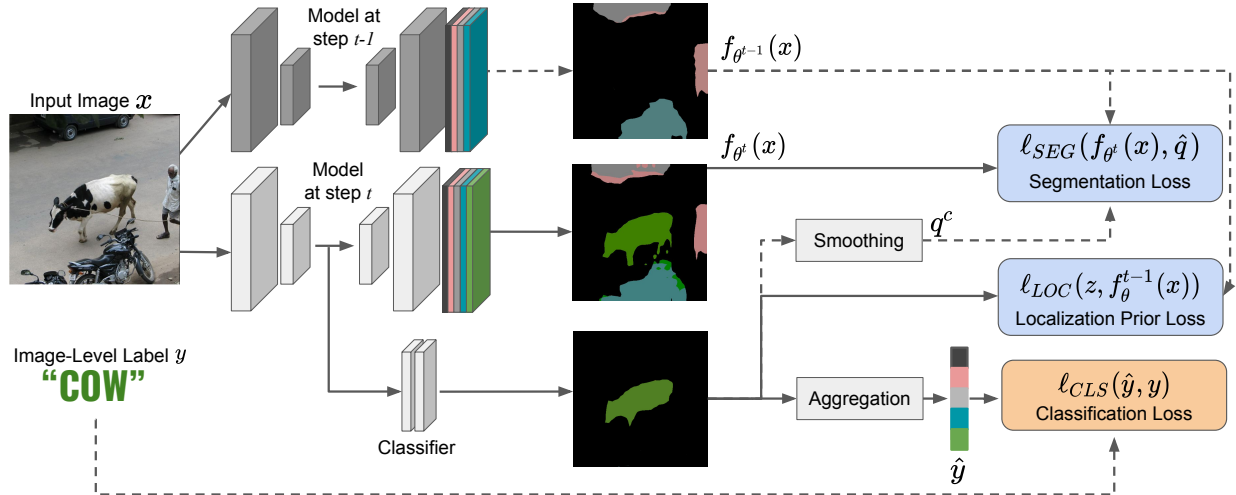


Figure 2. Illustration of the end-to-end training of WILSON. The auxiliary classifier is directly trained using a classification loss ℓ_{CLS} and the Localization Prior loss ℓ_{LOC} , which exploits the prior information of the old model at step $t-1$. The segmentation model is supervised using CAM and old model output. Gradient is not backpropagated on dotted lines.

ing incremental learning setting where we learn new classes over time, extending a pre-trained segmentation model using only image-level labels.

3. WILSON Framework

Adapting current WSSS methods [3, 34, 36, 37, 62] for incremental learning requires generating pseudo-labels offline for the new classes and then training a segmentation model separately. Instead, we propose an end-to-end framework for WILSS that can learn incrementally from pseudo-labels generated online by an auxiliary classifier attached to the model. In the following, we first define the problem and the notation (Sec. 3.1). Then we illustrate how the classification module can be trained to obtain pseudo-supervision (Sec. 3.2). Finally, in Sec. 3.3 we describe how to train the segmentation model to learn new classes without forgetting old ones. The framework is depicted in Fig. 2.

3.1. Problem Definition and Notation

We consider an input space \mathcal{X} (*i.e.* the image space) and assume, without loss of generality, that each image is composed by a set of pixels \mathcal{I} with constant cardinality $|\mathcal{I}| = H \times W = N$. The output space \mathcal{Y}^N is defined as the product set of N -tuples with elements in a label space \mathcal{Y} . In the standard semantic segmentation setting, given an image $x \in \mathcal{X}$, we want to learn a mapping to assign each pixel x_i a label $y_i \in \mathcal{Y}$, representing its semantic class. The mapping is realized by a model $f_\theta = d_{\theta^d} \circ e_{\theta^e} : \mathcal{X} \mapsto \mathbb{R}^{N \times |\mathcal{Y}|}$ from the image space \mathcal{X} to a pixel-wise class probability vector. e and d denote the encoder and decoder of the segmentation network, respectively. The output segmentation mask is obtained as $y^* = \{\arg \max_{c \in \mathcal{Y}} p_i^c\}_{i=1}^N$, where p_i^c is the model

prediction of pixel i for class c .

In the incremental segmentation setting [8], training is realized over multiple *learning steps*. At each learning step t , the previous label set \mathcal{Y}^{t-1} is augmented with novel classes \mathcal{C}^t , yielding a new label set $\mathcal{Y}^t = \mathcal{Y}^{t-1} \cup \mathcal{C}^t$. Differently from the original incremental setting, in WILSS we are provided with dense annotations only for the initial step ($t = 0$). That is, the model is pre-trained on a densely-annotated dataset $\mathcal{T}^0 \subset \mathcal{X} \times (\mathcal{C}^0)^N$ only for the initial classes. Then, for all the following steps we learn new classes only from cheap image-level labels. Namely, for ($t > 0$), we have access to multiple training sets with only image-level annotations for novel classes $\mathcal{T}^t \subset \mathcal{X} \times (\mathcal{C}^t)$. As in [8], we assume that data from previous training steps is not accessible anymore, and we want to update the model to perform segmentation on new classes preserving its performance on old classes *i.e.* $f_{\theta^t} : \mathcal{X} \mapsto \mathbb{R}^{N \times |\mathcal{Y}^t|}$.

3.2. Training the auxiliary classifier

Inspired by the WSSS literature [3, 5, 34, 36, 37, 62], we introduce an auxiliary classifier g , trained with image-level labels, to produce the pseudo-supervision for the segmentation model. The classifier uses the features from the segmentation encoder e to predict a score for all classes (background, old and new ones) *i.e.* $z = g(e(x)) \in \mathbb{R}^{|\mathcal{Y}^t| \times H \times W}$.

Learning from image-level labels. To learn from image-level labels first we need to aggregate the pixel-level classification scores z . The common solution is to use a Global Average Pooling (GAP) [3, 62]. However, simply averaging the scores produces coarse pseudo-labels [5], as all pixels in the feature map are encouraged to be less discriminative for the target class. For this reason, we use the *normalized*

Global Weighted Pooling (nGWP) [5], that weights every pixel based on its relevance for the target class. In particular, the weight of each pixel is computed normalizing the classification scores with the `softmax` operation ψ , i.e. $m = \psi(z)$. The aggregated scores are computed as:

$$\hat{y}^{nGWP} = \frac{\sum_{i \in I} m_i z_i}{\epsilon + \sum_{i \in I} m_i}, \quad (1)$$

where ϵ is a small constant. Moreover, to encourage the scores to identify all the visible parts of the object, we use the *focal penalty* term introduced by [5], that is obtained as:

$$\hat{y}^{FOC} = (1 - \frac{\sum_{i \in I} m_i}{|I|})^\gamma \log(\lambda + \frac{\sum_{i \in I} m_i}{|I|}), \quad (2)$$

where λ and γ are hyper-parameters. We refer the readers to [5] for more details on the nGWP and the focal penalty.

Since WILSS is an incremental learning scenario, we assume to have access only to image-level annotations y for the *new classes* \mathcal{C}^t . The classifier is then trained minimizing the *multi-label soft-margin loss*:

$$\ell_{CLS}(\hat{y}, y) = -\frac{1}{|\mathcal{K}|} \sum_{c \in \mathcal{K}} y^c \log(\hat{y}^c) + (1 - y^c) \log(1 - \hat{y}^c), \quad (3)$$

where $\mathcal{K} = \mathcal{C}^t$, $\hat{y} = \sigma(\hat{y}^{nGWP} + \hat{y}^{FOC})$, and σ is the logistic function. We note that, while the loss is computed only on new classes, it implicitly depends on the old classes scores due to the softmax-based aggregation in Eq. (1). However, since image-level annotations are cheap, and new images can be easily annotated, we may also consider a relaxed setting in which weak annotations are provide for both old and new classes. In this scenario the classification loss in Eq. (3) is computed on all classes and $\mathcal{K} = \mathcal{Y}^t$.

Localization Prior. The image-level labels provide supervision only on the presence of new classes in the image. However, they do not provide any cue on their boundaries or any information about the location of old classes. We argue that these insights can be freely obtained from the segmentation model learned in previous learning steps. In particular, the background score can be used as a saliency prior to extracting better object boundaries. Moreover, the scores of the old classes guide the auxiliary classifier in detecting whether and where an old class is present in the image, directing its attention to alternative regions.

Hence, we introduce a direct supervision on the classifier coming from the segmentation model trained on step $t-1$, i.e. f_θ^{t-1} . The supervision acts as a *Localization Prior* (LOC) and can be provided as a pixel-wise loss between the segmentation model outputs $\omega = \sigma(f_\theta^{t-1}(x))$ and the classification scores z . Formally, we minimize the following

objective function:

$$\ell_{LOC}(z, \omega) = -\frac{1}{|\mathcal{Y}^{t-1}| |I|} \sum_{i \in I} \sum_{c \in \mathcal{Y}^{t-1}} \omega_i^c \log(\sigma(z_i^c)) + (1 - \omega_i^c) \log(1 - \sigma(z_i^c)), \quad (4)$$

where $\sigma(\cdot)$ is the logistic function. In Eq. (4), the segmentation model provides dense a target on old classes. Unlike the `softmax` operator, which enforces competition among classes, the `logistic` function makes the class probabilities independent which is beneficial for a correct localization prior; in the case of a novel class, both old classes and the background will have a low score, implicitly informing the classifier that the pixel belongs to a new class.

3.3. Learning to Segment from Pseudo-Supervision

A solution often adopted by WSSS methods to train the semantic segmentation network is to extract hard-pseudo labels from an image-level classifier. In particular, these are obtained generating a one-hot distribution $q^{\text{Hard},c}$ for each pixel, attributing value one to the class with the maximum score for each pixel and zero to the others, i.e.

$$q_i^{\text{Hard},c} = \begin{cases} 1 & \text{if } c = \arg \max_{k \in \mathcal{Y}^t} m_i^k, \\ 0 & \text{otherwise,} \end{cases} \quad (5)$$

where m is the softmax normalized score extracted from the auxiliary classifier.

However, it is well-known that pseudo-supervision generated from an image-level classifier is noisy [5, 36, 37, 62], and using $q^{\text{Hard},c}$ to supervise the segmentation network may be detrimental for learning, causing the model to fit the wrong targets. For this reason, we propose to smooth the hard pseudo-labels based on m . Formally, given a class c , the pseudo-supervision q^c is computed as:

$$q^c = \alpha q^{\text{Hard},c} + (1 - \alpha) m^c, \quad (6)$$

where α is a hyper-parameter that controls the smoothness.

Although the auxiliary classifier produces scores for both new and old classes, the output distribution might be biased towards new classes due to the incremental training step. Thus, using q as a target for the segmentation model would lead to catastrophic forgetting [43]. Inspired by the knowledge distillation framework [28], we replace the pseudo-supervision extracted from the auxiliary classifier on old classes with the output of the segmentation model trained in the previous learning step. The final pixel-level pseudo-supervision \hat{q} is thus composed as follows:

$$\hat{q}^c = \begin{cases} \min(\sigma(f_{\theta^{t-1}}(x))^c, q^c) & \text{if } c = \mathbf{b}, \\ q^c & \text{if } c \in \mathcal{C}^t, \\ \sigma(f_{\theta^{t-1}}(x))^c & \text{otherwise,} \end{cases} \quad (7)$$

where b is the background class and $\sigma(\cdot)$ is the logistic function. We note that we utilize the minimum value of the two distributions for the background class, which contributes in modeling the background shift [8].

Since the pseudo-supervision q^c is not a probability distribution that sums to one, as required by the standard softmax-based cross-entropy loss, we propose to use a training loss based on the multi-label soft-margin loss:

$$\ell_{SEG}(p, \hat{q}) = -\frac{1}{|I|} \sum_{i \in I} \sum_{c \in \mathcal{Y}^t} \hat{q}_i^c \log(p_i^c) + (1 - \hat{q}_i^c) \log(1 - \sigma(p_i^c)), \quad (8)$$

where \mathcal{Y}^t is the set of all seen classes and $p = f_{\theta^t}(x)$ is the segmentation model output.

In conclusion, we remark that the auxiliary classifier is not employed during the testing phase, thus our method does not increase the time required for the inference.

4. Experiments

4.1. Datasets and Settings

We provide an extensive evaluation of WILSON on the two standard benchmarks Pascal VOC 2012 [23] and COCO [40]. Following the standard methodology [3, 34], we augment the Pascal VOC dataset with images from [26] for a total of 10582 images for training and 1449 for validation annotated on 20 object categories. COCO is a large-scale dataset providing 164K images and 80 object classes. We follow the training split and the annotation of [7] that solves the overlapping annotation problem present in [40].

Following prior works [8, 42], we adopt two incremental learning settings on the Pascal VOC dataset: the **15-5 VOC**, where 15 classes are learned in the first learning phase and 5 new classes added in a second step, and the **10-10 VOC**, where two steps of 10 classes are performed. Following [8, 42], we report results using two experimental protocols: (i) the *disjoint* scenario, in which each training step includes images containing only new or previously seen classes; (ii) the *overlap* scenario, in which each training step includes all the images containing at least one pixel from a novel class. In addition, we propose a novel incremental learning scenario, the **COCO-to-VOC**, composed of two training steps. First, we learn the 60 COCO classes not present in the Pascal VOC dataset, removing all the images containing at least one pixel of the latter. Then, in the second step, we learn 20 Pascal VOC classes. Following previous protocols [8, 42], we report the results on the dataset validation sets since the test set labels have not been publicly released. We adopt the standard mean Intersection over Union metric (mIoU) [23] to evaluate the performance of the segmentation model.

We recall that, differently from [8, 42], in the proposed WILSS setting the incremental steps provide only image-level labels for the new classes.

4.2. Baselines

Given that WILSS is a new setting, we compare WILSON with both incremental learning and weakly supervised semantic segmentation approaches. We report eight methods that represent the current state-of-the-art for incremental learning using pixel-wise supervision: LWF [38], LWF-MC [53], ILT [44], MiB [8], PLOP [21], CIL [33], SDR [45], and RECALL [42]. We note that RECALL [42], differently from other methods, uses additional images taken from the Web. For Pascal VOC, we use the results published in [21, 42], while we run the experiments on the COCO-to-VOC setting using the code provided by [8].

Furthermore, we report the performance of several state-of-the-art WSSS methods adapted to operate in the incremental learning scenario. In particular, we first train a classification model using the images available in the incremental learning steps. Then, we generate the hard pseudo-labels offline and train the segmentation model minimizing Eq. (8). We report the results with the pseudo-labels generated from: the class activation maps obtained from a standard image classifier (CAM), SEAM [62], SS [5], and EPS [36]. As for WILSON we followed the same experimental protocols provided by [8], training each method using only the images belonging to disjoint and overlap scenarios. For each method, we used the implementation released by the authors to produce the results. For CAM, we used the implementation of EPS to generate the pseudo-labels. It is important to remark that, while CAM, SS, and SEAM rely only on image-level labels, EPS also makes use of an off-the-shelf saliency detector trained on external data.

4.3. Implementation Details

We employ Deeplab V3 [13] architecture for all the experiments, with a ResNet-101 [27] backbone with output stride equal to 16 for Pascal VOC and a Wide-ResNet-38 [64] with output stride 8 for COCO, both pre-trained on ImageNet. As in [8], we use in-place activated batch normalization [55] to reduce the memory footprint required by the experiments. The auxiliary classifier used to generate the CAMs is composed of 3 convolutional layers followed by batch normalization and Leaky ReLU, where the first two have kernel size 3×3 while the last 1×1 , with channel numbers $\{256, 256, \text{number of classes}\}$, and stride 1. The model is trained for 40 epochs using batch size 24 and SGD with an initial learning rate of 0.001 (0.01 for the Deeplab head and the auxiliary classifier), momentum 0.9, and weight decay 10^{-4} . We train only the auxiliary classifier for the first 5 epochs. Then, we train the whole network by adding the pseudo-supervision from the classi-

Table 1. Results on the 15-5 setting of Pascal VOC expressed in mIoU%. The best method using Image-level supervision is bold. The best method using Pixel supervision is underlined. *: results from [42]. \diamond : results from [21].

Method	Sup	Disjoint			Overlap		
		1-15	16-20	All	1-15	16-20	All
Joint *	Pixel	75.5	73.5	75.4	75.5	73.5	75.4
FT *	Pixel	8.4	33.5	14.4	12.5	36.9	18.3
LWF * [38]	Pixel	39.7	33.3	38.2	67.0	41.8	61.0
LWF-MC * [53]	Pixel	41.5	25.4	37.6	59.8	22.6	51.0
ILT * [44]	Pixel	31.5	25.1	30.0	69.0	46.4	63.6
CIL * [33]	Pixel	42.6	35.0	40.8	14.9	37.3	20.2
MIB * [8]	Pixel	71.8	43.3	64.7	75.5	49.4	69.0
PLOP \diamond [21]	Pixel	71.0	42.8	64.3	<u>75.7</u>	51.7	70.1
SDR * [45]	Pixel	<u>73.5</u>	47.3	<u>67.2</u>	75.4	52.6	69.9
RECALL * [42]	Pixel	69.2	<u>52.9</u>	66.3	67.7	<u>54.3</u>	65.6
CAM	Image	67.5	25.5	57.8	68.6	24.9	58.6
SEAM [62]	Image	68.9	32.5	61.1	65.7	29.5	57.9
SS [5]	Image	68.9	25.9	60.2	71.4	27.2	61.5
EPS [36]	Image	70.7	36.8	63.6	67.8	33.7	60.7
WILSON (ours)	Image	72.0	44.1	66.3	73.2	43.0	66.8

Table 2. Results on the 10-10 setting of Pascal VOC expressed in mIoU%. The best method using Image-level supervision is bold. The best method using Pixel supervision is underlined. *: results from [42].

Method	Sup	Disjoint			Overlap		
		1-10	11-20	All	1-10	11-20	All
Joint *	Pixel	76.6	74.0	75.4	76.6	74.0	75.4
FT *	Pixel	7.7	60.8	33.0	7.8	58.9	32.1
LWF * [38]	Pixel	63.1	61.1	62.2	<u>70.7</u>	63.4	67.2
LWF-MC * [53]	Pixel	52.4	42.5	47.7	53.9	43.0	48.7
ILT * [44]	Pixel	<u>67.7</u>	<u>61.3</u>	<u>64.7</u>	70.3	61.9	66.3
CIL * [33]	Pixel	37.4	60.6	48.8	38.4	60.0	48.7
MIB * [8]	Pixel	66.9	57.5	62.4	70.4	63.7	67.2
SDR * [45]	Pixel	67.5	57.9	62.9	70.5	<u>63.9</u>	<u>67.4</u>
RECALL * [42]	Pixel	64.1	56.9	61.9	66.0	58.8	63.7
CAM	Image	64.8	41.2	54.2	69.7	43.9	57.8
SEAM [62]	Image	61.5	52.3	58.3	68.6	55.9	63.4
SS [5]	Image	60.3	27.2	45.5	69.7	33.6	52.9
EPS [36]	Image	64.3	53.8	60.5	68.6	56.6	63.8
WILSON (ours)	Image	64.2	54.5	60.8	70.5	56.9	64.9

fier and decay the learning rate using a polynomial schedule with a power of 0.9. Following [5], we set $\lambda = 0.01$, $\gamma = 3$ of Eq. (2), and after the fifth epoch, we use the self-supervised segmentation loss on the auxiliary classifier. Finally, we set $\alpha = 0.5$ in Eq. (6) for all the experiments.

4.4. Results

Single step addition of five classes (15-5). In this setting, after the initial learning stage, the following 5 classes of the VOC dataset are added: *plant, sheep, sofa, train, tv-monitor*. We report results in Tab. 1. Despite being trained only with image-level labels, WILSON achieves competitive results in all settings (disjoint and overlap) against approaches trained with pixel-wise supervision. Considering all the classes, in the disjoint scenario, we are able to

Table 3. Results on the COCO-to-VOC setting expressed in mIoU%. The best method using Image-level supervision is bold. The best method using Pixel supervision is underlined.

Method	Sup	COCO			VOC
		1-60	61-80	All	61-80
FT	Pixel	2.1	37.9	11.1	<u>72.2</u>
LWF [38]	Pixel	32.7	<u>47.4</u>	36.4	70.3
ILT [44]	Pixel	<u>36.9</u>	40.6	<u>37.8</u>	64.7
MIB [8]	Pixel	32.9	46.6	36.9	69.1
CAM	Image	30.7	20.3	28.1	39.1
SEAM [62]	Image	31.2	28.2	30.5	48.0
SS [5]	Image	35.1	36.9	35.5	52.4
EPS [36]	Image	34.9	38.4	35.8	55.3
WILSON (ours)	Image	36.9	37.9	37.2	56.8

match RECALL [42] performance, demonstrating the resilience of WILSON to forgetting without the need for a replay buffer while maintaining enough plasticity for learning new classes. Moreover, in the disjoint scenario, we surpass PLOP [21] by 1.3% and MIB [8] by 0.8% on new classes, while the difference between WILSON and SDR [45] is only of 3.2% points.

Considering WSSS methods adapted to the WILSS scenario, the results are a demonstration of the strengths of WILSON: the ability to retain the knowledge of past classes and, most importantly, the capability of learning new semantic classes given only image-level annotations. Indeed, when considering new classes, we outperform EPS [36] by +7.3% mIoU in the disjoint scenario, although it uses saliency maps generated from an external off-the-shelf model. Moreover, SEAM [62] is outperformed by 11.6% and SS [5] by 18.2%. These achievements are even more pronounced in the overlap scenario, where WILSON not only preserves all the prior knowledge but also achieves a +9.3% boost when learning new classes w.r.t. EPS. In this situation, the overall improvement is +5.3% when compared to the best result (SS).

Single step addition of ten classes (10-10). In this setting, we introduce 10 classes in the incremental step: *dining-table, dog, horse, motorbike, person, plant, sheep, sofa, train, tv-monitor*. Tab. 2 shows consistent results with the 15-5 setting. The differences between WILSON and IL (pixel-wise supervision) methods are quite small and the results are nearly comparable. In terms of accuracy, the gap using the most accurate incremental learning method, ILT, is 3.9% in the disjoint scenario and shrinks to 2.0% in the overlap one when compared to SDR. The efficacy of WILSON is confirmed when compared to the WSSS (image-level supervision) method as well. Indeed, while learning novel semantic classes, our online technique outperforms all offline competitors in the disjoint protocols by +0.7%, while achieving a comparable result in the overlap scenario. When measuring the mIoU on all classes, the ability to retain existing knowledge and to learn new classes is also

proven, with greater results than the EPS technique and a boost in the overlap scenario. In Fig. 3 we report qualitative results demonstrating the superiority of WILSON on both new and old classes.

COCO-to-VOC. This set of experiments can be considered the most challenging. Initially, the network is trained on 60 classes from the COCO dataset (which are not shared with VOC), while additional 20 classes from the VOC dataset are added in the second step. Tab. 3 shows evaluations on both COCO and VOC validation sets. Despite WILSON drops 10% when learning new classes compared to LwF, this experiment better showcases our ability to retain prior information while learning new classes under image-level supervision, matching ILT performance on old classes, which is the top competitor trained with pixel-wise supervision. When comparing against WSSS methods, WILSON is on average the best method, marking +1.4% improvements in terms of mIoU from the best WSSS method (EPS). Similar results hold also for the VOC validation set. We note that, while EPS slightly prevails on the new classes on COCO, WILSON outperforms it on both the old classes on COCO and on the new classes on VOC.

4.5. Ablation studies

Localization Prior. To validate the robustness of the pseudo-supervision generation, we perform an ablation study considering different choices for training the auxiliary classifier. Results are reported in Tab. 4 on the VOC 10-10 disjoint and overlap scenarios. In particular, we compare different strategies for training the auxiliary classifier: (i) we use a constant value for the old classes, as in [5], (ii) we use a fixed prior, directly concatenating the segmentation output of the old model to the class scores when computing m , (iii) we provide a localization supervision to the classifier with the softmax cross-entropy loss and (iv) with the loss in Eq. (4). Using a constant value and disregarding past knowledge from the old segmentation network results in lower performance when compared to the overall accuracy obtained if using a localization prior, particularly on old classes (-4.6% on both disjoint and overlap). This demonstrates that teaching the classifier the location of previous classes might be an effective way to prevent forgetting and improve performance while learning new classes. Thereby, using aggressive priors, such as directly using the segmentation output of the old model, does not allow the network to learn effectively the new classes, thus resulting in a gap of -4.2% on disjoint and -3.8% on overlapped scenario w.r.t. ℓ_{LOC} . Moreover, using the softmax cross-entropy loss to match the segmentation output is detrimental for the performance, achieving poor results on both new and old classes (-6.3% on disjoint and -5.2% on overlapped with respect to ℓ_{LOC}). The reason for this result is that, due

Table 4. Ablation study to validate the robustness of pseudo-supervision considering different types of localization priors for training the auxiliary classifier.

Prior	Loss	Disjoint			Overlap		
		1-10	11-20	All	1-10	11-20	All
-	-	64.8	49.9	58.8	69.4	52.0	62.0
Fixed	-	66.1	50.3	59.7	71.4	52.8	63.4
Learned	CE	61.1	46.0	54.5	67.6	49.5	59.2
Learned	ℓ_{LOC}	64.2	54.5	60.8	69.8	56.6	64.4

Table 5. Performance evaluation of weakly supervised segmentation methods trained with direct supervision on both old and new classes in the incremental step.

Method	VOC 15-5					
	Disjoint			Overlap		
	1-15	16-20	All	1-15	16-20	All
CAM	71.2	38.8	61.1	73.5	40.3	66.2
SEAM [62]	70.2	32.7	62.0	68.4	30.8	60.2
SS [5]	69.7	26.2	60.2	70.9	27.1	61.1
EPS [36]	72.6	46.2	67.2	73.6	46.6	68.0
WILSON (ours)	74.2	46.0	68.3	74.9	44.4	68.3

Method	VOC 10-10					
	Disjoint			Overlap		
	1-10	11-20	All	1-10	11-20	All
CAM	65.9	42.7	55.5	71.8	46.2	60.1
SEAM [62]	66.2	50.3	59.7	71.6	54.1	64.1
SS [5]	60.0	29.5	46.4	69.8	33.4	52.9
EPS [36]	68.3	51.1	61.0	72.0	55.4	65.4
WILSON (ours)	69.5	56.4	64.2	73.4	58.0	66.8

to the softmax normalization, the cross-entropy loss does not consider each class independently, and forces the classifier to produce high scores for old classes even when they have low segmentation scores.

Smoothing effect on pseudo-supervision. We tune the hyper-parameter α of Eq. (4), which regulates the smoothness of the pseudo-labels supervising the segmentation model. In Fig. 4 we show the final mIoU in the VOC 10-10 disjoint and overlap scenarios, for five distinct α values ranging from 0 to 1. As expected, in the case of $\alpha = 1$, which corresponds to using hard labels, the model fits the noise in the supervision, leading to worst results, forgetting the prior knowledge, and being incapable of learning novel classes. We chose $\alpha = 0.5$ for our experiment since it is a reasonable trade-off in accuracy between learning and remembering. It is crucial to note that changing the values from 0 to 0.7 affects the results by less than 0.5% on average between the disjoint and overlap case, indicating the robustness of WILSON to different α values.

Using supervision for all the classes. Since image-level supervision is cheap, we evaluate the performance of weakly-supervised methods when the supervision is provided for both old and new classes in the incremental steps. Tab. 5 reports the results on VOC. Comparing the results with Tab. 1 and Tab. 2, we note a performance improvement. In particular, all the methods improved, with WILSON

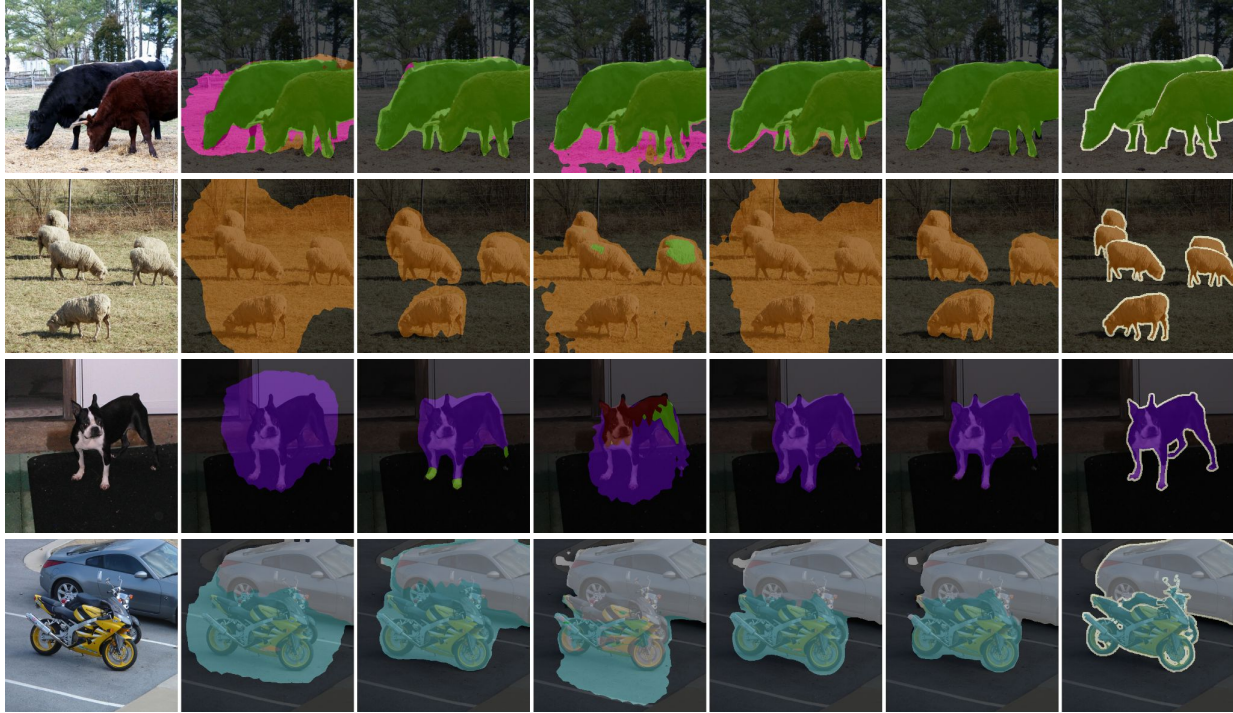


Figure 3. Qualitative results on the 10-10 VOC setting comparing different weakly supervised semantic segmentation methods. The image emphasized the efficiency of WILSON in both learning new classes (e.g. sheep, dog, motorbike) and preserving knowledge of old ones (e.g. cow, car). From left to right: image, CAM, SEAM [62], SS [5], EPS [36], WILSON and the ground-truth. Best viewed in color.

achieving, on average, 2% on both old and new classes on the 15-5 and 10-10. This result demonstrates that introducing knowledge about old classes in the pseudo-supervision generation is crucial to both learning new classes and avoiding forgetting. Moreover, we show that also in this scenario WILSON outperforms the offline WSSS methods. In particular, WILSON achieves better performance on every setting, outperforming EPS by 0.9% and 0.3% in the VOC 15-5 and by 3.2% and 1.4% in the VOC 10-10, respectively for the disjoint and overlapped scenario.

4.6. Limitations

Despite the remarkable results achieved by WILSON, it still has some drawbacks. To begin with, it is unable to perform single-class incremental learning steps, since Eq. 3 requires negative examples to properly guide the training. Moreover, we still need a considerable amount of images to train the model. Investigating learning from a few images could be an interesting future direction.

5. Conclusions

In this paper, we proposed WILSS, a novel setting that aims to extend the knowledge of semantic segmentation models through cheap image-level annotations. Applying current weakly-supervised learning approaches would re-

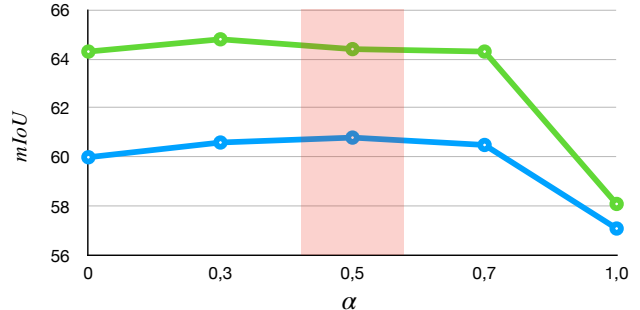


Figure 4. Ablation study about the effect of α to smooth the one-hot pseudo-labels used to supervise the ℓ_{SEG} . Test reporting the overall mIoU for both the **Disjoint** and **Overlap** protocols.

quire to generate the pseudo-supervision offline and then train the segmentation model. Differently, we propose WILSON, that couples the semantic segmentation model with an auxiliary classifier and use image-level annotations on the new classes to generate online the pseudo-supervision for the segmentation backbone. We show that adding a localization prior from the old model to the classifier improves the generation of the pseudo-labels. We prove the effectiveness of our approach in three incremental settings. We outperform the WSSS baselines that generate pseudo-labels offline and we get results close to fully supervised incremental learning methods.

References

- [1] Hongjoon Ahn, Jihwan Kwak, Subin Lim, Hyeonsu Bang, Hyojun Kim, and Taesup Moon. Ss-il: Separated softmax for incremental learning. In *Proceedings of the IEEE/CVF International Conference on Computer Vision*, pages 844–853, 2021. 2
- [2] Jiwoon Ahn, Sunghyun Cho, and Suha Kwak. Weakly supervised learning of instance segmentation with inter-pixel relations. In *Proceedings of the IEEE/CVF Conference on Computer Vision and Pattern Recognition*, pages 2209–2218, 2019. 2
- [3] Jiwoon Ahn and Suha Kwak. Learning pixel-level semantic affinity with image-level supervision for weakly supervised semantic segmentation. In *Proceedings of the IEEE Conference on Computer Vision and Pattern Recognition*, pages 4981–4990, 2018. 2, 3, 5
- [4] Emanuele Alberti, Antonio Tavera, Carlo Masone, and Barbara Caputo. Idda: a large-scale multi-domain dataset for autonomous driving. *IEEE Robotics and Automation Letters*, 5(4):5526–5533, 2020. 1
- [5] Nikita Araslanov and Stefan Roth. Single-stage semantic segmentation from image labels. In *Proceedings of the IEEE/CVF Conference on Computer Vision and Pattern Recognition*, pages 4253–4262, 2020. 2, 3, 4, 5, 6, 7, 8, 12, 15, 16, 17, 18, 19
- [6] Amy Bearman, Olga Russakovsky, Vittorio Ferrari, and Li Fei-Fei. What’s the point: Semantic segmentation with point supervision. In *European conference on computer vision*, pages 549–565. Springer, 2016. 1, 2
- [7] Holger Caesar, Jasper Uijlings, and Vittorio Ferrari. Coco-stuff: Thing and stuff classes in context. In *Proceedings of the IEEE conference on computer vision and pattern recognition*, pages 1209–1218, 2018. 5
- [8] Fabio Cermelli, Massimiliano Mancini, Samuel Rota Buló, Elisa Ricci, and Barbara Caputo. Modeling the background for incremental learning in semantic segmentation. In *Proceedings of the IEEE/CVF Conference on Computer Vision and Pattern Recognition*, pages 9233–9242, 2020. 1, 2, 3, 5, 6
- [9] Fabio Cermelli, Massimiliano Mancini, Yongqin Xian, Zeynep Akata, and Barbara Caputo. A few guidelines for incremental few-shot segmentation. *arXiv preprint arXiv:2012.01415*, 2020. 2
- [10] Yu-Ting Chang, Qiaosong Wang, Wei-Chih Hung, Robinson Piramuthu, Yi-Hsuan Tsai, and Ming-Hsuan Yang. Weakly-supervised semantic segmentation via sub-category exploration. In *Proceedings of the IEEE/CVF Conference on Computer Vision and Pattern Recognition*, pages 8991–9000, 2020. 2
- [11] Arslan Chaudhry, Puneet K Dokania, Thalaiyasingam Ajanthan, and Philip HS Torr. Riemannian walk for incremental learning: Understanding forgetting and intransigence. In *Proceedings of the European Conference on Computer Vision (ECCV)*, pages 532–547, 2018. 2
- [12] Arslan Chaudhry, Puneet K Dokania, and Philip HS Torr. Discovering class-specific pixels for weakly-supervised semantic segmentation. *arXiv preprint arXiv:1707.05821*, 2017. 2
- [13] Liang-Chieh Chen, George Papandreou, Iasonas Kokkinos, Kevin Murphy, and Alan L Yuille. Deeplab: Semantic image segmentation with deep convolutional nets, atrous convolution, and fully connected crfs. *IEEE TPAMI*, 40(4):834–848, 2017. 1, 2, 5
- [14] Liang-Chieh Chen, George Papandreou, Florian Schroff, and Hartwig Adam. Rethinking atrous convolution for semantic image segmentation. 2017. 1, 2
- [15] Liang-Chieh Chen, Yukun Zhu, George Papandreou, Florian Schroff, and Hartwig Adam. Encoder-decoder with atrous separable convolution for semantic image segmentation. In *ECCV*, 2018. 1, 2
- [16] Bowen Cheng, Omkar Parkhi, and Alexander Kirillov. Pointly-supervised instance segmentation. *arXiv preprint arXiv:2104.06404*, 2021. 1
- [17] Marius Cordts, Mohamed Omran, Sebastian Ramos, Timo Rehfeld, Markus Enzweiler, Rodrigo Benenson, Uwe Franke, Stefan Roth, and Bernt Schiele. The cityscapes dataset for semantic urban scene understanding. In *Proc. of the IEEE Conference on Computer Vision and Pattern Recognition (CVPR)*, 2016. 1
- [18] Jifeng Dai, Kaiming He, and Jian Sun. Boxesup: Exploiting bounding boxes to supervise convolutional networks for semantic segmentation. In *Proceedings of the IEEE international conference on computer vision*, pages 1635–1643, 2015. 1, 2
- [19] Jia Deng, Wei Dong, Richard Socher, Li-Jia Li, Kai Li, and Li Fei-Fei. Imagenet: A large-scale hierarchical image database. In *2009 IEEE conference on computer vision and pattern recognition*, pages 248–255. Ieee, 2009. 1
- [20] Prithviraj Dhar, Rajat Vikram Singh, Kuan-Chuan Peng, Ziyang Wu, and Rama Chellappa. Learning without memorizing. In *Proceedings of the IEEE/CVF Conference on Computer Vision and Pattern Recognition*, pages 5138–5146, 2019. 2
- [21] Arthur Douillard, Yifu Chen, Arnaud Dapogny, and Matthieu Cord. Plop: Learning without forgetting for continual semantic segmentation. In *Proceedings of the IEEE/CVF Conference on Computer Vision and Pattern Recognition*, pages 4040–4050, 2021. 1, 2, 5, 6
- [22] Arthur Douillard, Matthieu Cord, Charles Ollion, Thomas Robert, and Eduardo Valle. Podnet: Pooled outputs distillation for small-tasks incremental learning. In *Computer Vision—ECCV 2020: 16th European Conference, Glasgow, UK, August 23–28, 2020, Proceedings, Part XX 16*, pages 86–102. Springer, 2020. 2
- [23] Mark Everingham, Luc Van Gool, Christopher K. I. Williams, John M. Winn, and Andrew Zisserman. The pascal visual object classes (voc) challenge. *International Journal of Computer Vision*, 88:303–338, 2009. 1, 2, 5, 12
- [24] Enrico Fini, Stéphane Lathuilière, Enver Sangineto, Moin Nabi, and Elisa Ricci. Online continual learning under extreme memory constraints. In *European Conference on Computer Vision*, pages 720–735. Springer, 2020. 2
- [25] Robert M French. Catastrophic forgetting in connectionist networks. *Trends in cognitive sciences*, 3(4), 1999. 2

- [26] Bharath Hariharan, Pablo Arbeláez, Lubomir Bourdev, Subhransu Maji, and Jitendra Malik. Semantic contours from inverse detectors. In *2011 International Conference on Computer Vision*, pages 991–998. IEEE, 2011. 5
- [27] Kaiming He, Xiangyu Zhang, Shaoqing Ren, and Jian Sun. Deep residual learning for image recognition. In *CVPR*, pages 770–778, 2016. 5
- [28] Geoffrey Hinton, Oriol Vinyals, and Jeff Dean. Distilling the knowledge in a neural network. 2015. 4
- [29] Qibin Hou, Peng-Tao Jiang, Yunchao Wei, and Ming-Ming Cheng. Self-erasing network for integral object attention. *arXiv preprint arXiv:1810.09821*, 2018. 2
- [30] Xinting Hu, Kaihua Tang, Chunyan Miao, Xian-Sheng Hua, and Hanwang Zhang. Distilling causal effect of data in class-incremental learning. In *Proceedings of the IEEE/CVF Conference on Computer Vision and Pattern Recognition*, pages 3957–3966, 2021. 2
- [31] Zilong Huang, Xinggong Wang, Jiayi Wang, Wenyu Liu, and Jingdong Wang. Weakly-supervised semantic segmentation network with deep seeded region growing. In *Proceedings of the IEEE Conference on Computer Vision and Pattern Recognition*, pages 7014–7023, 2018. 2
- [32] Anna Khoreva, Rodrigo Benenson, Jan Hosang, Matthias Hein, and Bernt Schiele. Simple does it: Weakly supervised instance and semantic segmentation. In *Proceedings of the IEEE conference on computer vision and pattern recognition*, pages 876–885, 2017. 1, 2
- [33] Marvin Klingner, Andreas Bär, Philipp Donn, and Tim Fingscheidt. Class-incremental learning for semantic segmentation re-using neither old data nor old labels. In *2020 IEEE 23rd International Conference on Intelligent Transportation Systems (ITSC)*, pages 1–8. IEEE, 2020. 2, 5, 6
- [34] Alexander Kolesnikov and Christoph H Lampert. Seed, expand and constrain: Three principles for weakly-supervised image segmentation. In *European conference on computer vision*, pages 695–711. Springer, 2016. 1, 2, 3, 5
- [35] Jungbeom Lee, Eunji Kim, Sungmin Lee, Jangho Lee, and Sungroh Yoon. Ficklenet: Weakly and semi-supervised semantic image segmentation using stochastic inference. In *Proceedings of the IEEE conference on computer vision and pattern recognition*, pages 5267–5276, 2019. 2
- [36] Seungho Lee, Minhyun Lee, Jongwuk Lee, and Hyunjung Shim. Railroad is not a train: Saliency as pseudo-pixel supervision for weakly supervised semantic segmentation. In *Proceedings of the IEEE/CVF Conference on Computer Vision and Pattern Recognition*, pages 5495–5505, 2021. 2, 3, 4, 5, 6, 7, 8, 15, 16, 17, 18, 19
- [37] Yi Li, Zhanghui Kuang, Liyang Liu, Yimin Chen, and Wayne Zhang. Pseudo-mask matters in weakly-supervised semantic segmentation. In *Proceedings of the IEEE/CVF International Conference on Computer Vision*, pages 6964–6973, 2021. 3, 4
- [38] Zhizhong Li and Derek Hoiem. Learning without forgetting. *IEEE transactions on pattern analysis and machine intelligence*, 40(12):2935–2947, 2017. 2, 5, 6
- [39] Di Lin, Jifeng Dai, Jiaya Jia, Kaiming He, and Jian Sun. Scribblesup: Scribble-supervised convolutional networks for semantic segmentation. In *Proceedings of the IEEE conference on computer vision and pattern recognition*, pages 3159–3167, 2016. 1, 2
- [40] Tsung-Yi Lin, Michael Maire, Serge Belongie, James Hays, Pietro Perona, Deva Ramanan, Piotr Dollár, and C Lawrence Zitnick. Microsoft coco: Common objects in context. In *European conference on computer vision*, pages 740–755. Springer, 2014. 1, 2, 5, 12
- [41] Yaoyao Liu, Yuting Su, An-An Liu, Bernt Schiele, and Qianru Sun. Mnemonics training: Multi-class incremental learning without forgetting. In *Proceedings of the IEEE/CVF conference on Computer Vision and Pattern Recognition*, pages 12245–12254, 2020. 2
- [42] Andrea Maracani, Umberto Michieli, Marco Toldo, and Pietro Zanuttigh. Recall: Replay-based continual learning in semantic segmentation. In *Proceedings of the IEEE/CVF International Conference on Computer Vision*, pages 7026–7035, 2021. 1, 2, 5, 6
- [43] Michael McCloskey and Neal J Cohen. Catastrophic interference in connectionist networks: The sequential learning problem. In *Psychology of learning and motivation*, volume 24, pages 109–165. Elsevier, 1989. 1, 2, 4
- [44] Umberto Michieli and Pietro Zanuttigh. Incremental learning techniques for semantic segmentation. In *ICCV-WS*, pages 0–0, 2019. 1, 2, 5, 6
- [45] Umberto Michieli and Pietro Zanuttigh. Continual semantic segmentation via repulsion-attraction of sparse and disentangled latent representations. In *Proceedings of the IEEE/CVF Conference on Computer Vision and Pattern Recognition*, pages 1114–1124, 2021. 1, 2, 5, 6
- [46] Umberto Michieli and Pietro Zanuttigh. Knowledge distillation for incremental learning in semantic segmentation. *Computer Vision and Image Understanding*, 205:103167, 2021. 2
- [47] Seong Joon Oh, Rodrigo Benenson, Anna Khoreva, Zeynep Akata, Mario Fritz, and Bernt Schiele. Exploiting saliency for object segmentation from image level labels. In *2017 IEEE conference on computer vision and pattern recognition (CVPR)*, pages 5038–5047. IEEE, 2017. 2
- [48] George Papandreou, Liang-Chieh Chen, Kevin P Murphy, and Alan L Yuille. Weakly-and semi-supervised learning of a deep convolutional network for semantic image segmentation. In *Proceedings of the IEEE international conference on computer vision*, pages 1742–1750, 2015. 2
- [49] Deepak Pathak, Philipp Krahenbuhl, and Trevor Darrell. Constrained convolutional neural networks for weakly supervised segmentation. In *Proceedings of the IEEE international conference on computer vision*, pages 1796–1804, 2015. 1
- [50] David Patterson, Joseph Gonzalez, Quoc Le, Chen Liang, Lluís-Miquel Munguia, Daniel Rothchild, David So, Maud Texier, and Jeff Dean. Carbon emissions and large neural network training. *arXiv preprint arXiv:2104.10350*, 2021. 1
- [51] Pedro O Pinheiro and Ronan Collobert. From image-level to pixel-level labeling with convolutional networks. In *Proceedings of the IEEE conference on computer vision and pattern recognition*, pages 1713–1721, 2015. 1

- [52] Rui Qian, Yunchao Wei, Honghui Shi, Jiachen Li, Jiaying Liu, and Thomas Huang. Weakly supervised scene parsing with point-based distance metric learning. In *Proceedings of the AAAI Conference on Artificial Intelligence*, volume 33, pages 8843–8850, 2019. [2](#)
- [53] Sylvestre-Alvise Rebuffi, Alexander Kolesnikov, Georg Sperl, and Christoph H Lampert. icarl: Incremental classifier and representation learning. In *Proceedings of the IEEE conference on Computer Vision and Pattern Recognition*, pages 2001–2010, 2017. [2](#), [5](#), [6](#)
- [54] Stephan R. Richter, Vibhav Vineet, Stefan Roth, and Vladlen Koltun. Playing for data: Ground truth from computer games. In Bastian Leibe, Jiri Matas, Nicu Sebe, and Max Welling, editors, *European Conference on Computer Vision (ECCV)*, volume 9906 of *LNCS*, pages 102–118. Springer International Publishing, 2016. [1](#)
- [55] Samuel Rota Bulò, Lorenzo Porzi, and Peter Kotschieder. In-place activated batchnorm for memory-optimized training of dnns. In *CVPR*, 2018. [5](#)
- [56] Hanul Shin, Jung Kwon Lee, Jaehong Kim, and Jiwon Kim. Continual learning with deep generative replay. *arXiv preprint arXiv:1705.08690*, 2017. [2](#)
- [57] Emma Strubell, Ananya Ganesh, and Andrew McCallum. Energy and policy considerations for deep learning in nlp. *arXiv preprint arXiv:1906.02243*, 2019. [1](#)
- [58] Guolei Sun, Wenguan Wang, Jifeng Dai, and Luc Van Gool. Mining cross-image semantics for weakly supervised semantic segmentation. In *European conference on computer vision*. Springer, 2020. [2](#)
- [59] Meng Tang, Abdelaziz Djelouah, Federico Perazzi, Yuri Boykov, and Christopher Schroers. Normalized cut loss for weakly-supervised cnn segmentation. In *Proceedings of the IEEE Conference on Computer Vision and Pattern Recognition*, pages 1818–1827, 2018. [2](#)
- [60] Neil C Thompson, Kristjan Greenewald, Keeheon Lee, and Gabriel F Manso. The computational limits of deep learning. *arXiv preprint arXiv:2007.05558*, 2020. [1](#)
- [61] Paul Vernaza and Manmohan Chandraker. Learning random-walk label propagation for weakly-supervised semantic segmentation. In *Proceedings of the IEEE conference on computer vision and pattern recognition*, pages 7158–7166, 2017. [1](#)
- [62] Yude Wang, Jie Zhang, Meina Kan, Shiguang Shan, and Xilin Chen. Self-supervised equivariant attention mechanism for weakly supervised semantic segmentation. In *Proceedings of the IEEE/CVF Conference on Computer Vision and Pattern Recognition*, pages 12275–12284, 2020. [2](#), [3](#), [4](#), [5](#), [6](#), [7](#), [8](#), [15](#), [16](#), [17](#), [18](#), [19](#)
- [63] Yunchao Wei, Jiashi Feng, Xiaodan Liang, Ming-Ming Cheng, Yao Zhao, and Shuicheng Yan. Object region mining with adversarial erasing: A simple classification to semantic segmentation approach. In *Proceedings of the IEEE conference on computer vision and pattern recognition*, pages 1568–1576, 2017. [2](#)
- [64] Zifeng Wu, Chunhua Shen, and Anton Van Den Hengel. Wider or deeper: Revisiting the resnet model for visual recognition. *Pattern Recognition*, 90:119–133, 2019. [5](#)
- [65] Yazhou Yao, Tao Chen, Guo-Sen Xie, Chuanyi Zhang, Fumin Shen, Qi Wu, Zhenmin Tang, and Jian Zhang. Non-salient region object mining for weakly supervised semantic segmentation. In *Proceedings of the IEEE/CVF Conference on Computer Vision and Pattern Recognition*, pages 2623–2632, 2021. [2](#)
- [66] Bolei Zhou, Aditya Khosla, Agata Lapedriza, Aude Oliva, and Antonio Torralba. Learning deep features for discriminative localization. In *Proceedings of the IEEE conference on computer vision and pattern recognition*, pages 2921–2929, 2016. [2](#)
- [67] Fei Zhu, Xu-Yao Zhang, Chuang Wang, Fei Yin, and Cheng-Lin Liu. Prototype augmentation and self-supervision for incremental learning. In *Proceedings of the IEEE/CVF Conference on Computer Vision and Pattern Recognition (CVPR)*, pages 5871–5880, June 2021. [2](#)

Supplementary Material

A. Additional Implementation Details

This section, provides additional implementation details on the training of the auxiliary classifier introduced in the WILSON framework. We recall that the auxiliary classifier, denoted as g , takes as input the features coming from the segmentation encoder e to predict a score for all classes (background, old and new ones) *i.e.* $z = g(e(x)) \in \mathbb{R}^{|\mathcal{Y}^t| \times H \times W}$, where \mathcal{Y}^t is the set of classes seen (new and old) at the incremental step t . In the main paper, we described two loss functions (the classification loss ℓ_{CLS} and the localization prior ℓ_{LOC}) that we used to train the classifier. However, for the sake of space, we left to the supplementary material two additional losses.

Pixel-wise refinement of the auxiliary classifier output. Following [5], we introduced a self-supervised segmentation loss on the auxiliary classifier output. This loss aims to force classification scores to be locally consistent, *i.e.* near pixels with similar appearance should be assigned the same classification score. First, we apply a refinement process on the classification output based on the pixel-level image similarity. Then, we force the classification scores to be similar to the refined version by using a pixel-level segmentation loss only on the auxiliary classifier without directly affecting the segmentation output.

To refine the classification scores, similarly to [5], we employ the *Pixel Adaptive Mask Refinement* (PAMR). PAMR is a parameter-free module that iteratively refines the score of each pixel. Starting from the normalized classification score $m = \psi(z)$, PAMR refines it by considering the neighbour pixels $N(i)$. We initialize $m^{ref,0} = m$ and, at the t^{th} iteration the refined mask $m^{ref,t}$ is computed as:

$$m_i^{ref,t} = \sum_{n \in N(i)} \alpha_{i,n} \cdot m^{ref,t-1}(n), \quad (9)$$

where the pixel-level level affinity $\alpha_{i,n}$ is a value that measures the similarity among two pixels which is computed using a kernel function k on the pixel intensities, so that:

$$\alpha_{i,n} = \frac{e^{k(i,n)}}{\sum_{l \in N(i)} e^{k(i,l)}}, \quad (10)$$

where we followed the same definition of the kernel function k defined in [5] that considers the average similarity in pixel intensity on the RGB channels. As suggested in [5], we used 3×3 neighborhood with different dilation rates, that we set to $\{1, 2, 4, 8, 12\}$, and we stopped after 10 iterations. Please refer to [5] for additional details.

The refined classification scores are then converted to a pseudo ground-truth mask to compute the self-supervised segmentation loss. We ignored clashing pixels and we selected only pixels with a confidence higher than 60% of

the maximum value (greater than 70% for the background class). The auxiliary classifier is then trained by optimizing a weighted cross-entropy loss:

$$\ell_{SSS} = - \sum_{i \in I} \sum_{c \in \mathcal{Y}^t} w_c \log m_{c,i} \quad (11)$$

with $w_c = \frac{|I| - M_c}{1 + |I|}$ and $M_c = \sum_{i \in I} m_{c,i}^{ref}$, indicating with c, i the score of class c at pixel i .

Encoder feature distillation loss. Since the losses applied on the auxiliary classifier are backpropagated on the segmentation encoder, it is possible that they will cause a shift in encoder representation, impacting negatively the segmentation performance.

We use an additional *feature distillation loss* to prevent the encoder’s representation from shifting towards new classes and forgetting old ones. In particular, we used a *mean-squared error* function between the features extracted by the current encoder e^t , and the ones extracted at previous step e^{t-1} . Formally, given an image x , the loss is computed as:

$$\ell_{ENC} = \frac{1}{|I|} \sum_{i \in I} (e^t(x)_i - e^{t-1}(x)_i)^2, \quad (12)$$

where I is the set of pixels in the image and the suffix indicates the value at pixel i .

Overall training procedure. To sum up, the auxiliary classifier has been trained, for the first 5 epochs, to minimize the following loss function:

$$\ell_{TOT_{B5}} = \lambda_1 \ell_{CLS} + \lambda_2 \ell_{LOC} + \lambda_3 \ell_{ENC}, \quad (13)$$

where $\lambda_1, \lambda_2, \lambda_3$ are all set to 1.

After the fifth epoch, we introduce the self-supervised segmentation loss, as in [5]:

$$\ell_{TOT_{A5}} = \lambda_1 \ell_{CLS} + \lambda_2 \ell_{LOC} + \lambda_3 \ell_{ENC} + \lambda_4 \ell_{SSS}, \quad (14)$$

with $\lambda_4 = 1$.

Code. The code to replicate WILSON has been attached to the supplementary material. The code provides the scripts to replicate WILSON and the baselines for all the settings. For the offline weakly-supervised methods, we refer to the official implementations^{2 3 4} to generate the pseudo-labels.

B. Detailed results

B.1. Dataset class splits

We provide an extensive evaluation of WILSON on the two standard benchmarks Pascal VOC 2012 [23] and COCO [40]. Following previous work, we used two data

²<https://github.com/YudeWang/SEAM>

³<https://github.com/halbielee/EPS>

⁴<https://github.com/visinf/1-stage-wseg>

settings on Pascal VOC: 15-5 and 10-10. To split the dataset, we follow the standard practice, and we divide them according to the alphabetic order. Tab. 6 and Tab. 7 report the classes for the 15-5 and 10-10 settings, respectively. For the COCO dataset, we split the classes according to their presence in the Pascal VOC dataset. In particular, classes in the Pascal VOC dataset are in the incremental step, while the others are in the base one. The split is reported in Tab. 8.

B.2. Class-by-class results

In this section, we report per class results on all the settings considered in the main paper. We considered the off-line weakly supervised methods (WSSS) as baselines. At the same time, we could not report values for the incremental learning methods since these are not available in the considered published works.

Single step addition of five classes (15-5). In Tab. 9 and Tab. 10 are reported the results for the disjoint and overlapped settings, respectively. From the tables, we can see that WILSON outperforms all the WSSS baselines on most of the classes. In particular, considering the disjoint setting, it obtains better results on 11 out of 15 old classes and 4 out of 5 novel ones. On the overlapped, WILSON obtains even better results, being best on 12 out of 15 old classes and all the new ones. Moreover, in comparison with the joint training with pixel-level supervision, it achieves close results and, surprisingly, even superior on some old classes (*e.g.*, *bike*, *boat*, *bottle*, *d.table*). Differently, on the new classes, we still note a considerable performance gap, especially on classes with highly variable shapes, such as *plant*.

Single step addition of five classes (10-10). Tab. 11 and Tab. 12 report the results for the disjoint and overlapped settings. In this more challenging setting, the performance gap between WILSON and the WSSS baselines is reduced, but WILSON still obtains better results on the majority of the classes. In particular, WILSON outperforms the baselines on 3 and 4 out of 10 old classes in the disjoint and overlapped scenario, respectively, and on 4 out of 10 new classes in both scenarios. The difficulty of the setting is also confirmed by the comparison with the Joint training baseline. In particular, in the disjoint setting, WILSON achieves 10.9% less mIoU on old classes and 24.7% on the new ones, while in the overlapped setting, the performance improves on the old classes (-5.1% mIoU) but decreases on the new ones (-17.1%).

The difficulty of the setting is also proven by the comparison with the Joint training baseline. In particular, in the disjoint setting WILSON achieves 10.9% less mIoU on old classes and 24.7% on the new ones. In the overlapped, the performance improves on the old classes (-5.1% mIoU) but decreases on the new ones (-17.1%).

COCO-to-VOC. COCO-to-VOC is the most challenging

Table 6. Pascal VOC 15-5 class split.

step	classes
0	aeroplane, bicycle, bird, boat, bottle, bus, car, cat, chair, cow, table, dog, horse, motorbike, person
1	plant, sheep, sofa, train, tv-monitor

Table 7. Pascal VOC 10-10 class split.

step	classes
0	aeroplane, bicycle, bird, boat, bottle, bus, car, cat, chair, cow
1	table, dog, horse, motorbike, person, plant, sheep, sofa, train, tv-monitor

Table 8. COCO class split.

step	classes
0	truck, traffic light, fire hydrant, stop sign, parking meter, bench, elephant, bear, zebra, giraffe, backpack, umbrella, handbag, tie, suitcase, frisbee, skis, snowboard, sports ball, kite, baseball bat, baseball glove, skateboard, surfboard, tennis racket, wine glass, cup, fork, knife, spoon, bowl, banana, apple, sandwich, orange, broccoli, carrot, hot dog, pizza, donut, cake, bed, toilet, laptop, mouse, remote, keyboard, cell phone, microwave, oven, toaster, sink, refrigerator, book, clock, vase, scissors, teddy bear, hair drier, toothbrush
1	person, bicycle, car, motorcycle, airplane, bus, train, boat, bird, cat, dog, horse, sheep, cow, bottle, chair, couch, potted plant, dining table, tv

scenario proposed in the paper. Not only the classes to learn are more, but they also come from different datasets, *i.e.* COCO on the base step and Pascal VOC on the incremental one. We report the results on the incremental classes on VOC on Tab. 13. From the results, we see that WILSON obtains the best results, outperforming SS (the second best) by 1.5% mIoU. Moreover, it achieves better results than the WSSS baselines on 8 out of 20 classes. The results on the COCO dataset are reported in Tab. 14. We note that the most challenging classes are small objects that often appear with the person class, such as *skii*, *handbag*, *baseball bat*, *skateboard*, *toaster*, *hair-drier*. The low performances can be explained considering that, at step 0, we removed from COCO all the images containing at least a pixel from a class of VOC, including *person*, significantly reducing the number of samples occurring often with it (*e.g.*, *skateboard*, *skii*)

and compromising their performances.

C. Additional Qualitative Results

In the main paper, we reported qualitative results for the VOC 10-10 setting. We introduce additional qualitative results here, showing results for each setting (VOC 15-5 and COCO-to-VOC) and some failure cases.

Single step addition of five classes (15-5). Fig. 5 shows evaluations on the Pascal VOC 15-5 setting in which five classes are added in a single step. As we can see from the images, WILSON predictions on new classes *sofa*, *train* and *tv-monitor* are much more accurate than those produced by EPS, even if the latter exploits an off-the-shelf saliency detector to better capture object shapes. The performances are even higher than CAM, SEAM, and SS, which tend to extend the new class predictions over the background pixels inaccurately. On old classes, WILSON is significantly more resilient to catastrophic forgetting than the other competitors, being able to properly segment both *boat* and *cat* pixels. It is also worth noting that WILSON is the only approach capable of accurately classifying the majority of the old class *boat* pixels, avoiding the uncertainty towards the class *train* that the other competitors manifest.

COCO-to-VOC. Fig. 6 and Fig. 7 provide the results on COCO-to-VOC setting in which additional 20 VOC classes are added in a second step, respectively evaluating each method on VOC and COCO validation sets. Fig. 6 confirms the strong performances on newer classes observed in the VOC 15-5 and 10-10 settings, demonstrating how only WILSON is able to segment the leg of the motorcyclist and the background of the *chair* with significantly fewer inaccuracies than the others competitors. The results achieved on *plant* category show the ability of WILSON in successfully segmenting small objects as well, compared to EPS which entirely fails in accurately predicting small object boundaries. Even on the COCO validation dataset, WILSON outperforms the other state-of-the-art weakly-supervised semantic segmentation methods, as shown in Fig. 7. Indeed, it is able to segment the old classes *umbrella*, *sandwich*, *parking meter* and the new ones *person*, *dog*, *cat*, *tv-monitor* with much less uncertainty. Both CAM and SS perform poorly in this scenario, while SEAM and EPS still show some misclassified pixels. We also note that none of the provided approaches can classify the *tennis racket* correctly. We attribute this behavior to a context bias, as many training images involve a person holding a skateboard, and the models have learned to associate a person holding *something* to a *skateboard*.

Failure Modes. Finally, Fig. 8 reports some failure cases and inaccurate predictions of each method. The first situation in which WILSON exhibits difficulties is in separating the object from its context. Indeed, like with the *table-chair*

pair in VOC 15-5, *monitor-keyboard* in VOC 10-10, and *tv-monitor-furniture* in COCO-to-VOC (VOC), it includes in the prediction of the main class also objects that are commonly observed together. The second flaw regards object boundaries. WILSON as shown in VOC 15-5, is unable to appropriately segment each boundary of the new class *plant*, whereas EPS is able to do so. The same trend may be seen in COCO-to-VOC (VOC) *boat*. Finally, WILSON demonstrates the final failure in terms of misclassified predictions between old and new classes. It mixes the old class *sheep* with the new class *cow*, as illustrated in VOC 10-10. Furthermore, it confuses *truck* and *car* in COCO-to-VOC (COCO).

Table 9. Per class results on the Pascal VOC 15-5 Disjoint setting, expressed in mIoU. Best Image-supervised method in bold.

Method	Sup	bkg	aplane	bike	bird	boat	bott	bus	car	cat	chair	cow	d.table	dog	horse	mbike	person	plant	sheep	sofa	train	tv	Old	New	All
Joint	Pixel	92.5	89.9	39.2	87.6	65.2	77.3	91.1	88.5	92.9	34.8	84.0	53.7	88.9	85.0	85.1	84.9	60.0	79.7	47.0	82.2	73.5	76.5	68.5	75.4
CAM	Image	76.9	72.9	39.5	75.6	53.7	74.9	71.2	86.5	89.1	29.6	35.5	54.0	82.1	82.0	82.2	82.9	19.4	15.7	26.3	29.6	33.9	67.5	25.0	57.8
SEAM [62]	Image	83.7	77.3	36.3	79.7	40.8	64.8	69.6	81.0	85.4	30.1	64.7	48.8	81.4	81.3	78.0	82.2	14.6	32.8	30.5	37.1	33.2	68.9	32.5	61.1
SS [5]	Image	86.3	75.8	38.9	82.6	62.4	75.4	73.0	86.9	88.4	29.8	59.2	53.4	77.7	82.6	79.5	83.4	18.2	23.5	20.7	24.7	42.4	69.9	25.9	60.2
EPS [36]	Image	90.0	84.3	40.8	83.8	63.4	75.2	77.6	86.8	88.4	31.2	43.5	55.2	85.2	82.7	80.9	82.0	21.1	39.3	23.3	61.3	39.1	70.7	36.8	63.6
WILSON (Ours)	Image	90.9	89.1	41.3	85.3	67.6	78.4	76.5	89.1	90.5	32.7	47.3	57.5	84.9	84.5	70.6	85.2	28.1	47.4	38.8	57.4	48.9	72.0	44.1	66.3

Table 10. Per class results on the Pascal VOC 15-5 Overlapped setting, expressed in mIoU. Best Image-supervised method in bold.

Method	Sup	bkg	plane	bike	bird	boat	bottle	bus	car	cat	chair	cow	d.table	dog	horse	m.bike	person	plant	sheep	sofa	train	tv	Old	New	All
Joint	Pixel	92.5	89.9	39.2	87.6	65.2	77.3	91.1	88.5	92.9	34.8	84.0	53.7	88.9	85.0	85.1	84.9	60.0	79.7	47.0	82.2	73.5	76.5	68.5	75.4
CAM	Image	77.1	69.6	39.7	70.0	57.6	75.4	58.4	86.8	89.0	33.2	60.3	57.9	84.2	78.4	85.0	84.2	17.2	15.6	26.0	32.1	33.4	68.6	24.9	58.6
SEAM [62]	Image	82.8	73.2	36.9	67.7	25.0	62.9	17.9	79.3	88.4	32.7	69.5	49.9	83.4	71.0	73.8	83.7	12.0	31.4	29.7	30.4	28.7	65.7	29.5	57.9
SS [5]	Image	84.6	77.5	38.4	78.4	58.1	75.3	73.0	85.8	87.5	35.3	72.8	57.0	83.0	81.4	82.8	84.2	13.0	27.8	22.8	33.3	39.1	71.4	27.2	61.5
EPS [36]	Image	89.6	77.1	39.0	79.8	62.8	77.5	31.9	85.8	87.7	34.2	57.9	57.2	85.2	76.5	80.8	83.9	17.3	40.6	26.1	45.1	39.2	67.8	33.7	60.7
WILSON (Ours)	Image	90.7	87.3	42.1	87.5	69.0	78.8	70.4	89.7	91.0	37.1	62.2	59.1	87.8	82.1	68.0	86.1	26.3	47.7	36.9	58.2	45.8	73.2	43.0	66.8

Table 11. Per class results on the Pascal VOC 10-10 Disjoint setting, expressed in mIoU. Best Image-supervised method in bold.

Method	Sup	bkg	aplane	bike	bird	boat	bott	bus	car	cat	chair	cow	d.table	dog	horse	mbike	person	plant	sheep	sofa	train	tv	Old	New	All
Joint	Pixel	92.5	89.9	39.2	87.6	65.2	77.3	91.1	88.5	92.9	34.8	84.0	53.7	88.9	85.0	85.1	84.9	60.0	79.7	47.0	82.2	73.5	75.1	74.0	75.4
CAM	Image	78.3	85.8	35.5	77.4	62.4	77.1	78.6	78.4	73.6	23.1	56.1	39.5	41.0	29.5	49.0	47.9	38.6	37.6	35.2	49.6	44.1	64.8	41.2	54.2
SEAM [62]	Image	86.5	82.7	37.2	81.0	61.8	76.4	66.0	45.9	77.4	25.4	60.9	42.5	66.4	48.2	64.8	56.3	30.3	68.5	36.5	56.2	53.0	61.5	52.3	58.3
SS [5]	Image	81.2	78.8	25.0	83.6	60.5	80.1	81.4	66.7	61.3	25.6	39.8	21.0	19.2	8.8	24.2	24.3	31.6	38.5	21.7	39.0	43.6	60.3	27.2	45.5
EPS [36]	Image	88.6	86.6	35.3	83.9	66.1	77.7	61.0	65.3	78.1	27.1	62.4	40.9	64.4	52.9	67.9	65.8	42.5	46.3	39.8	74.6	42.5	64.3	53.8	60.5
WILSON (Ours)	Image	89.8	80.4	32.7	87.1	54.2	79.6	76.0	68.3	79.1	28.4	56.3	31.6	68.1	45.8	62.9	59.3	46.4	70.4	39.5	63.9	57.1	64.2	59.3	62.9

Table 12. Per class results on the Pascal VOC 10-10 Overlapped setting, expressed in mIoU. Best Image-supervised method in bold.

Method	Sup	bkg	aplane	bike	bird	boat	bott	bus	car	cat	chair	cow	d.table	dog	horse	mbike	person	plant	sheep	sofa	train	tv	Old	New	All
Joint	Pixel	92.5	89.9	39.2	87.6	65.2	77.3	91.1	88.5	92.9	34.8	84.0	53.7	88.9	85.0	85.1	84.9	60.0	79.7	47.0	82.2	73.5	75.1	74.0	75.4
CAM	Image	78.3	81.9	38.4	84.0	64.8	77.1	82.9	86.1	82.6	30.8	68.2	38.5	50.6	40.0	52.8	48.0	38.6	38.2	36.8	50.1	44.8	69.7	43.9	57.8
SEAM [62]	Image	87.2	84.1	37.7	84.4	64.2	78.0	76.8	76.9	83.1	30.6	70.2	42.0	73.0	59.2	68.1	60.4	36.8	69.1	43.9	56.2	50.1	68.6	55.9	63.4
SS [5]	Image	78.9	86.0	39.1	85.0	66.9	77.6	87.8	85.2	78.1	32.8	58.4	20.9	41.4	31.3	41.0	22.6	31.0	38.2	25.3	39.6	44.3	69.7	33.6	52.9
EPS [36]	Image	88.5	84.6	38.7	85.5	66.3	78.8	66.4	77.7	83.6	32.7	71.4	37.3	75.3	62.4	71.9	66.7	42.3	50.3	42.0	76.1	41.9	68.6	56.6	63.8
WILSON (Ours)	Image	89.1	83.3	37.9	87.4	65.3	80.5	78.2	84.1	85.2	33.5	70.0	25.8	77.3	66.1	74.3	60.1	41.5	65.6	40.9	57.4	60.4	70.5	56.9	64.9

Table 13. Per class results on Pascal VOC for the COCO-to-VOC setting, expressed in mIoU. Best method in bold.

Method	Sup	bkg	person	bike	car	mbike	aplane	bus	train	boat	bird	cat	dog	horse	sheep	cow	bott	chair	sofa	plant	d.table	tv	All
CAM	Image	68.5	49.4	22.9	16.1	54.0	37.8	24.3	51.0	31.7	47.7	40.4	39.8	49.4	45.2	40.2	50.1	22.8	22.5	39.4	33.4	34.5	39.1
SEAM [62]	Image	76.3	65.8	26.1	42.6	60.9	54.9	9.7	51.3	30.9	76.6	63.3	60.2	52.7	47.1	59.0	22.9	28.9	40.2	37.4	37.2	48.0	
SS [5]	Image	81.8	71.2	34.8	33.7	71.3	80.7	41.7	77.5	57.2	81.1	69.2	65.6	65.0	51.3	51.4	63.7	27.6	22.8	49.5	26.4	37.8	55.3
EPS [36]	Image	79.9	70.2	29.0	43.1	65.3	63.2	44.3	60.7	42.4	78.6	70.3	64.6	64.4	32.2	49.4	68.1	28.2	30.0	49.4	24.9	42.6	52.4
WILSON (Ours)	Image	87.0	80.7	61.8	31.3	73.0	79.9	29.3	57.3	58.3	83.3	69.4	61.8	68.4	49.1	44.7	61.9	38.7	23.4	47.0	22.0	65.4	56.8

Table 14. Per class results on COCO for the COCO-to-VOC setting, expressed in mIoU. Best method in bold. VOC classes in red.

Method	Old	New	All	bkg	truck	traffic-light	fire-hydrant	stop-sign	parking-meter	bench	elephant	bear	zebra	giraffe	backpack	umbrella	handbag	tie	suitcase	frisbee
CAM	30.7	20.3	28.1	73.8	18.3	43.7	57.4	87.5	35.2	29.3	77.2	57.4	78.7	66.3	10.5	35.6	2.0	3.1	47.8	0.8
SEAM	31.2	28.2	30.5	81.2	15.8	40.3	67.5	86.4	35.7	30.7	77.3	61.6	86.8	79.1	12.0	39.6	2.4	3.5	44.9	1.4
SS	35.1	36.9	35.5	81.4	13.1	47.1	68.9	90.9	46.0	28.0	75.4	46.1	89.3	77.0	11.0	33.9	2.1	3.6	46.2	0.6
EPS	34.9	38.4	35.8	82.7	13.7	49.4	67.5	90.9	43.6	29.2	77.3	49.9	87.3	75.9	10.2	36.3	2.1	3.8	45.7	1.1
WILSON (Ours)	36.9	37.9	37.2	82.5	12.8	52.9	80.3	91.0	50.3	31.8	74.1	47.3	89.5	79.7	11.0	38.2	0.5	2.8	47.7	0.5
					skis	snowboard	sports-ball	kite	baseball-bat	baseball-glove	skateboard	surfboard	tennis-racket	wine-glass	cup	fork	knife	spoon	bowl	banana
					0.0	0.4	5.9	31.9	0.0	12.9	1.5	27.0	15.8	25.1	36.4	26.3	15.2	10.8	40.0	44.0
					0.0	0.4	5.1	30.8	0.0	6.6	0.8	25.7	12.2	28.7	33.7	22.2	12.4	7.0	39.3	39.7
					0.0	0.8	1.6	29.2	0.0	13.5	0.9	27.0	20.2	18.2	29.2	26.3	14.4	9.7	34.6	53.1
					0.0	0.3	5.2	27.6	0.0	5.5	1.1	28.2	14.5	19.8	31.8	25.4	12.4	10.4	34.3	52.8
					0.1	0.2	3.9	29.1	0.0	17.0	2.0	25.5	20.3	22.8	34.9	27.2	16.3	11.8	35.4	56.7
					apple	sandwich	orange	broccoli	carrot	hot-dog	pizza	donut	cake	bed	toilet	laptop	mouse	remote	keyboard	cell-phone
					33.7	30.5	48.7	33.9	35.4	29.1	55.7	39.0	35.1	14.5	54.7	35.8	22.2	8.1	37.8	35.3



Figure 5. Qualitative results on the 15-5 VOC setting comparing different weakly supervised semantic segmentation methods. From left to right: image, CAM, SEAM [62], SS [5], EPS [36], WILSON and the ground-truth. Best viewed in color.



Figure 6. Qualitative results on the COCO-to-VOC setting evaluated on VOC validation set. From left to right: image, CAM, SEAM [62], SS [5], EPS [36], WILSON and the ground-truth. Best viewed in color.



Figure 7. Qualitative results on the COCO-to-VOC setting evaluated on COCO validation set. From left to right: image, CAM, SEAM [62], SS [5], EPS [36], WILSON and the ground-truth. Best viewed in color.

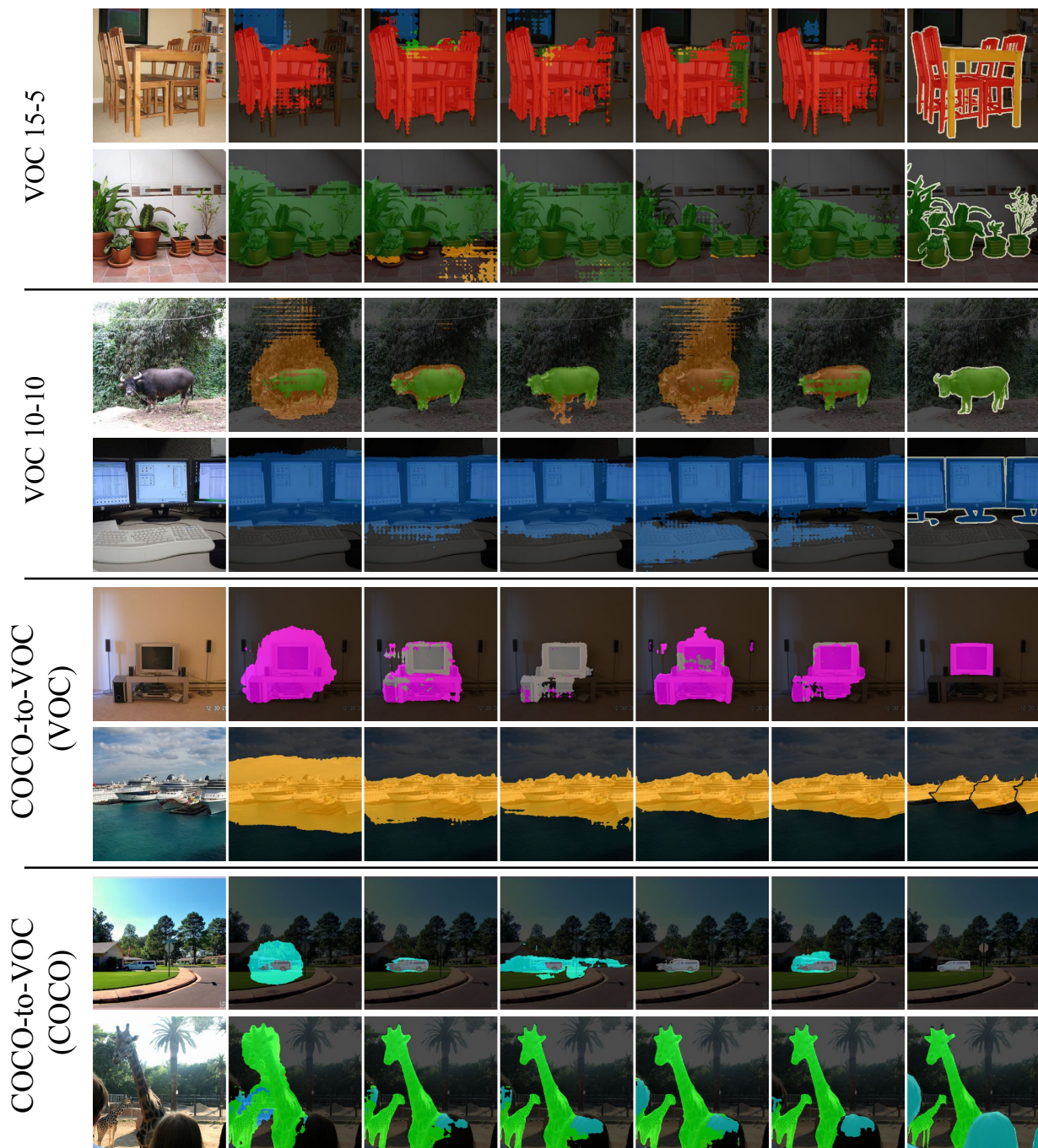


Figure 8. Qualitative results of failure on each setting, in order: VOC 15-5, VOC 10-10, COCO-to-VOC (VOC validation set) and COCO-to-VOC (COCO validation set). From left to right: image, CAM, SEAM [62], SS [5], EPS [36], WILSON and the ground-truth. Best viewed in color.